Archives of Environmental Protection
Vol. 52 no. 2 pp. 118–129

PL ISSN 2083-4772
DOI: 10.24425/aep.2026.1298

Competitive adsorption of pharmaceuticals from multicomponent solutions on functionalized mesoporous silica: comparing β-cyclodextrin and amine surface modifications

Lidia Bandura[1], Monika Białoszewska[1], Rafał Panek[1], Jacek Czerwiński[2], Tiina Leiviskä[3], Wojciech Franus*[1]

[1]Lublin University of Technology, Faculty of Civil Engineering and Architecture, Department of Building Materials Engineering and Geoengineering, Lublin, Poland
[2]Lublin University of Technology, Faculty of Environmental Engineering and Energy, Lublin, Poland
[3]Chemical Process Engineering, University of Oulu, Oulu FIN-90014, Finland

*Corresponding author's e-mails: w.franus@pollub.pl

Keywords: β-cyclodextrin, wastewater treatment, mesoporous silica, surface functionalization, pharmaceutical adsorption, competitive adsorption.

Abstract: The article compares the effectiveness of removing ibuprofen (IBU), sulfamethoxazole (SMX), and tetracycline (TC) from their mixture using mesoporous silica SBA-15 modified with β-cyclodextrin (CD) and aminosilane (APTES). SBA-15 was synthesized using a waste solution from the synthesis of zeolites from fly ash as a source of silicon. X-ray diffraction (XRD), CHN elemental analysis, Fourier transform infrared spectroscopy (FT-IR), N_2 adsorption isotherms, and scanning electron microscopy (SEM) were performed to obtain structural, chemical, and surface characteristics of the hybrid materials. Batch adsorption tests were performed to evaluate adsorbent-adsorbate interactions and competition between adsorbates at pH 6.5 and 9.0. Among the tested pharmaceuticals, TC showed the highest adsorption capacity, which indicates its greater affinity resulting from the presence of numerous functional groups that enable interactions with the adsorbent surface. The highest adsorption capacity qe for TC was 186.5 mg/g and 100.9 mg/g for SBA-15-CD and SBA-15-APTES, respectively, whereas the qe values for IBU and SMX were similar, amounting to ~ 150 mg/g and ~ 71 mg/g, respectively, at pH 6.5. SBA-15-CD showed similar removal efficiency at both tested pH values, whereas SBA-15-APTES clearly lost its affinity for the adsorbates at pH 9.0, where qe value for SMX decreased by approx. 20% compared with that at pH 6.5. The results indicate the high potential of waste-derived functionalized SBA-15 for the treatment of water and wastewater contaminated with pharmaceuticals.

Introduction

Pharmaceuticals represent a large and diverse group of bioactive chemical compounds commonly used in human medicine, veterinary medicine and livestock production, including their use as growth stimulants (Kim et al., 2020). Global emissions of pharmaceuticals are constantly increasing, leading to their increased release into the aquatic environment (Włodarczyk-Makuła, 2024). The main routes of entry include municipal and industrial wastewater from the medical, pharmaceutical, cosmetic and agricultural sectors (Sim et al., 2011). These compounds subsequently enter conventional wastewater treatment plants, where, as indicated in the literature, their removal is often insufficient (Ajaz et al., 2024; Kilpinen et al., 2024). As a result, pharmaceuticals are detected in surface water, groundwater and even drinking water (Kilpinen et al., 2024). Although the concentrations of these pollutants are usually in the range of μg/L to low mg/L, their continuous presence poses a serious threat to ecosystems and public health (Samal et al., 2022). Pharmaceuticals can bioaccumulate and affect the physiological processes of aquatic organisms, leading to ecosystem imbalances. They have been shown to exert toxic effects on bacteria, algae, fish and other aquatic organisms, and the presence of antibiotics further promotes the development and spread of antimicrobial resistance (Tang et al., 2025). This phenomenon has been recognized by the WHO as one of the most serious threats to public health in the 21st century (Walsh et al., 2023).

Pharmaceuticals classified as emerging contaminants, including ibuprofen (IBU), sulfamethoxazole (SMX), and tetracycline (TC), are widely recognized as problematic

pollutants due to their incomplete removal in conventional wastewater treatment processes and their continuous release into the aquatic environment. IBU is a widely used nonsteroidal anti-inflammatory drug (NSAID), whereas SMX and TC are antibiotics belonging to the sulfonamide and tetracycline groups, respectively, and are commonly used in human and veterinary medicine (Sim et al., 2011). These compounds enter the environment mainly through excretion, incomplete removal in wastewater treatment plants, and agricultural runoff, and are considered pseudo-persistent pollutants due to their continuous release and biological activity. In particular, antibiotics such as SMX and TC contribute to the development of antimicrobial resistance (Walsh et al., 2023), whereas IBU has been associated with measurable ecotoxicological effects in aquatic organisms (Huynh et al., 2023).

In view of the growing environmental burden posed by pharmaceuticals, it is crucial to develop effective and economically viable methods for their removal from wastewater, including sorption materials with high selectivity and sorption capacity. At the same time, systematic monitoring of their presence in water is necessary to reduce the risk of long-term adverse effects on both the environment and human health. Among highly efficient and selective sorbents, chemically modified materials that combine the properties of inorganic carriers with the functionality of organic groups are of particular interest (Abegunde et al., 2020; Amalina et al., 2022). A promising approach for the effective removal of contaminants with diverse polarity and chemical structures is the surface modification of adsorbents, including the use of β-cyclodextrin (β-CD) (Abukhadra, 2024; Bandura et al., 2021; Lagiewka et al., 2025; Poulson et al., 2022) and 3-aminopropyl triethoxysilane (APTES) (Caicedo et al., 2020; Nguyen et al., 2025).

β-Cyclodextrin (β-CD) is a cyclic oligosaccharide composed of seven glucopyranose units linked by α-1,4 glycosidic bonds. This structure forms a unique cone-shaped cavity with a hydrophobic interior and a hydrophilic outer surface, enabling the formation of inclusion complexes with hydrophobic and aromatic molecules through a host-guest mechanism driven mainly by van der Waals and hydrophobic interactions and stabilized by hydrogen bonding (Syeda et al., 2022). Owing to these properties, β-CD and its derivatives are highly effective in binding poorly water-soluble organic micropollutants, including pharmaceuticals, pesticides, and endocrine disruptors (Bandura et al., 2021; Wang et al., 2025; Xiang Chuin et al., 2024). Chemical immobilization (grafting) of β-CD onto inorganic carriers, such as mesoporous silica or zeolites, significantly enhances the stability and reusability of the material while preserving accessible inclusion sites. As previous studies have shown, the structure of the mineral carrier strongly influences the final properties of the resulting hybrid materials (Baigorria et al., 2024; Bandura et al., 2022; Mallard et al., 2015).

3-Aminopropyl triethoxysilane (APTES) is one of the most commonly used organosilanes for the modification of silica-based materials. It introduces $–NH_2$ groups onto the surface of the material, increasing its affinity for selected contaminants through hydrogen bonding, electrostatic interactions, or coordination with electron-rich groups (Cavalcante et al., 2022). Such functionalization can also make sorption pH-dependent, allowing greater selectivity in complex aqueous matrices (Althumayri et al., 2023). As comparative studies have shown, β-CD-modified materials often exhibit strong affinity toward hydrophobic and aromatic pollutants, whereas APTES modification can enhance interactions with more polar and/or ionic molecules (Flores et al., 2023). Therefore, a direct comparison of β-CD- and APTES-modified sorbents provides valuable insight into how different surface chemistries influence adsorption selectivity and capacity for diverse classes of contaminants. In addition to surface functionalization, the sustainability of sorbents can be further improved by designing their inorganic carriers through waste valorization.

This study aimed to evaluate the effectiveness of removing IBU, SMX, and TC from multicomponent solutions using mesoporous silica SBA-15 modified with β-cyclodextrin (SBA-15-CD) and 3-aminopropyltriethoxysilane (SBA-15-APTES). SBA-15 was obtained using a silicon-rich waste solution from the production of zeolites derived from fly ash (Panek et al., 2021), which is in line with the principles of sustainable development and supports the implementation of a circular economy strategy. The study analyzed the influence of functional groups on adsorption properties under competitive conditions and identified sorption mechanisms in the tested system.

Materials and methods

Materials and reagents

Pluronic P123 and HCl used for SBA-15 synthesis were purchased from Sigma Aldrich. The source of silica was solely the post-reaction solution obtained after the synthesis of zeolites from fly ash (Panek et al., 2021). Cyclodextrins (α, β, and γ), (3-Glycidyloxypropyl)trimethoxysilane (GLYMO), N, N-Dimethylformamide (DMF), and metallic sodium (Na), used for mesoporous silica functionalization, were obtained from Merck (Darmstadt, Germany). Pharmaceutical compounds (TC, SMX, and IBU; purity ≥99%) were obtained from Sigma-Aldrich (St. Louis, MO, USA). LC-MS-grade solvents (methanol, acetonitrile, formic acid) and analytical standards for QTOF-MS calibration were supplied by Merck (Darmstadt, Germany).

Sorbents preparation

The SBA-15 silica material was synthesized as follows: 12 g of Pluronic P123 surfactant was dissolved in 400 ml of deionized water, and 160 ml of concentrated hydrochloric acid was added. The solution was then placed on a magnetic stirrer, heated, and stirred for 1 hour. After this time, 400 ml of post-reaction solution was added to the mixture. The resulting suspension was stirred for 1 hour and aged for 24 hours at 40°C and for another 24 hours at 100°C. The solid phase was separated by filtration, rinsed, and dried at 105°C. The final product was calcined at 550°C for 6 hours.

The obtained SBA-15 was subsequently modified using two different approaches: (i) β-cyclodextrin (β-CD) grafting and (ii) 3-aminopropyltriethoxysilane (APTES) functionalization, as follows:

(i) β- Cyclodextrin (3 g) was dissolved in 100 mL of N,N-dimethylformamide (DMF) under magnetic stirring, followed by the addition of 0.3 g of metallic Na. After stirring for 2 h at room temperature, the suspension was filtered to remove

unreacted Na, and 2 mL (3-glycidyloxypropyl)trimethoxysilane (GLYMO) was added. The mixture was stirred at 85–90°C for 5 h, after which 3 g of SBA-15 was introduced and reacted at 90–100°C for 10 h. The product was filtered, sequentially washed with DMF, distilled water, methanol, and acetone, and dried at 105°C for 24 h.

(ii) Dried mesoporous silica (2 g) was suspended in 178 mL toluene, and 8.8 mL APTES was added. The mixture was refluxed at 100°C for 24 h, then filtered, washed with toluene, distilled water, and acetone, and dried at 105°C for 24 h.

Materials characterization

Phase composition was analyzed by powder XRD using a Panalytical X'PertPRO MPD (Almelo, the Netherlands) diffractometer with a PW 3050/60 goniometer, CuKα radiation (λ = 0.154178 nm), and a PIXcel1D detector. Data were collected in the 2θ range of 0.5–20 °2θ with a step size of 0.013° and a counting time of 80 s per step. Diffraction patterns were processed using X'Pert Highscore, and phase identification was based on the PDF-2 (2022) database of the JCPDS/ICDD.

Morphology was examined using a Quanta 250 FEG SEM (FEI, Hillsboro, Oregon, USA.) equipped with a LaB_6 electron source and an EDAX EDS detector. Samples were mounted on aluminum stubs with carbon tape and sputter-coated with carbon using a Quorum Q150T coater. Analyzes were performed in high-vacuum mode at an accelerating voltage of 10–15 kV.

Elemental analysis was carried out by energy-dispersive X-ray fluorescence (EDXRF) using a Panalytical Epsilon 3 spectrometer (Almelo, the Netherlands), equipped with a Rh anode X-ray tube (9 W, 50 kV, 1 mA), a 4096-channel analyzer, six primary filters (Cu-500, Cu-300, Ti, Al-50, Al-200, Ag), and a Peltier-cooled SDD detector. Powdered samples dried to constant weight were analyzed in the Na–Am range. CHN elements determination was performed on the CHN/CHNS EuroEA3000 Analyzer (EuroVector).

FTIR spectra were recorded on a Nicolet 380 spectrometer (Thermo Scientific, Waltham, Massachusetts, USA) in the range 4000–400 cm^{-1} at room temperature, with a resolution of 4 cm^{-1} and 256 scans per spectrum. Spectra were normalized against a KBr background without further smoothing.

Textural parameters were determined from N_2 adsorption–desorption isotherms at 77 K using a Micromeritics ASAP 2020 analyzer (Norcross, Atlanta, USA) in the relative pressure range $p/p_0 = 8\times10^{-8}$–0.13. Specific surface area (S_{BET}) was calculated using the BET method, while pore volume and size distribution were derived from adsorption data. Samples were degassed prior to analysis under the following conditions: SBA-15: 300 °C, 24 h; SBA-15-CD: 70 °C, 24 h; SBA-15-APTES: 100 °C, 24 h.

pH_{pzc} was determined by the pH drift method in 0.01 M NaCl, and calculated as the intersection point where the initial and final pH values were equal after equilibration.

Batch adsorption tests

Batch adsorption experiments were carried out to investigate the removal of IBU, SMX, and TC from multicomponent aqueous solutions. A stock solution was prepared by dissolving 0.2 g of each compound in 1 L of deionized water. Working solutions with concentrations ranging from 5 to 100 mg/L were prepared by appropriate dilutions. For each experiment, 50 mL of solution was placed in conical flasks, to which 25 mg of sorbent was added. The solid-to-liquid ratio was 0.5 g/L. The suspensions were maintained at room temperature under static conditions overnight to reach adsorption equilibrium. Experiments were conducted at pH 6.5 and pH 9.0 to reflect wastewater-relevant conditions in Poland; pH was adjusted to the target value at the start and monitored thereafter. After adsorption, the suspensions were centrifuged twice at 10,000 rpm for 10 min. The supernatants were collected and filtered through 0.22 μm PTFE syringe filters prior to HPLC-qTOF analysis. All experiments were performed in duplicate, and mean values are reported.

HPLC-qTOF analysis

Quantitative analysis of IBU, SMX, and TC was performed using an Agilent HPLC-qTOF system (Santa Clara, California, USA) consisting of a quaternary gradient pump (1260 Infinity II), a thermostated autosampler, a column oven maintained at 30 °C, and a Q-TOF 6546 mass spectrometer with an electrospray ionization (ESI) source operating in positive ion mode. Chromatographic separation was achieved on an Eclipse Plus C18 column (4.6 × 250 mm, 5 μm) with an injection volume of 5 μL. The mobile phase consisted of solvent A (0.1% formic acid in water, HPLC grade) and solvent B (0.1% formic acid in methanol, LC-MS grade). The elution program was as follows: 0–3 min, 10–70% B; 3–4 min, 70–98% B; 4–9 min, 98% B (isocratic); after 9 min, B was reduced to 10% and the system was re-equilibrated for 15 min. The flow rate was 0.5 mL/min. Mass spectrometric detection was performed with the following parameters: capillary voltage −4.7 kV, ion source temperature 350 °C, sheath gas pressure 45 psi, and gas flow 13.0 L/min. Instrumental conditions were optimized using Agilent Optimizer software to maximize signal response and lower instrumental detection limits (IDL). Quantification was based on the intensity of the protonated molecular ions $[M+H]^+$, while $[M+Na]^+$ and, in some cases, $[M+K]^+$ were used as confirmatory ions. Calibration curves were constructed for each pharmaceutical compound within the concentration ranges of 0.10–10 mg/L for IBU and 0.01–0.10 mg/L for SMX and TC, with coefficients of determination (R^2) ≥ 0.998. Limits of detection (LOD) and quantification (LOQ), determined based on signal-to-noise ratios (S/N) of 3 and 10, were in the range of 0.04–3.4 μg/L and 0.15–11.2 μg/L. A summary of analytical parameters is provided in Table 1.

Adsorption data analysis

For each solute *i* (IBU, SMX, TC), the removal (R_i, %) and equilibrium capacity ($q_{e,i}$, mg/g) were calculated as follows:

$$R_i(\%) = \frac{C_{0,i} - C_{e,i}}{C_{0,i}} \cdot 100$$

$$q_{e,i} = \frac{(C_{0,i} - C_{e,i})V}{m}$$

where $C_{0,i}$ and $C_{e,i}$ (mg/L) are the initial and equilibrium concentrations, respectively, V (L) is the solution volume, and m (g) is the sorbent mass.

For the multicomponent systems, the adsorption behavior of each pharmaceutical was described using the distribution coefficient (K_d, L/g), calculated as:

Table 1: Analytical parameters and validation data for HPLC–qTOF method

Ana0 lyte	Exact mass (m/z)	Precursor ion $[M+H]^+$ (m/z)	Confirmatory ion $[M+Na]^+$ (m/z)	Mass accuracy (±)	Calibration range (mg L^{-1})	R^2	Calibration equation	LOD (µg L^{-1})	LOQ (µg L^{-1})
IBU	206.130680	207.1385	229.1204	0.0003–0.0004	0.10–10.0	≥0.998	y = 1.634E−2x + 1.895E−5	0.04–3.4	0.15–11.2
SMX	253.052112	254.0599	276.0419	0.0004–0.0005	0.01–0.10	≥0.998	y = 1.737E−2x + 4.441E−4	0.04–3.4	0.15–11.2
TC	444.1533	445.1610	467.1430	0.0006–0.0007	0.01–0.10	≥0.998	y = 7.999E−6x	0.04–3.4	0.15–11.2

$$K_{d,i}\frac{q_{e,i}}{C_{e,i}}$$

where $q_{e,i}$ (mg/g) and $C_{e,i}$ (mg/L) are the equilibrium adsorption capacity and aqueous concentration of compound *i*, respectively.

The selectivity coefficient α between compounds *i* and *j* was then obtained as:

$$\alpha_{i/j}=\frac{K_{d,i}}{K_{d,j}}$$

so that values greater than 1 indicate preferential adsorption of compound *i* over *j*.

All coefficients were determined separately for each pH and equilibrium concentration. Selected multicomponent isotherm models (e.g., extended Langmuir model) were tested for fitting. However, the obtained fits were physically unrealistic or inconsistent with the experimental data. This behavior is consistent with literature reports for complex multicomponent systems, where conventional isotherm models often fail to adequately describe competitive adsorption due to overlapping mechanisms and non-ideal interactions (Acharya et al., 2023).

Results and discussion

Materials characterization

The SBA-15, SBA-15-CD and SBA-15-APTES diffractograms (Figure 1a) show a characteristic low-angle reflection (100) at 0.9 °2θ with corresponding interplanar distances (d_{hkl} = 97.18; 52.00; 34.23 Å). This clearly indicates that the SBA-15 phase was preserved in all tested samples after the functionalization process, which is consistent with research on the functionalization of SBA-15 using APTES and organic compounds (Mohassel Yazdi and Naimi-Jamal, 2024) XRF analysis confirmed that SBA-15 consists mainly of silica (SiO_2). CHN elemental analysis revealed a significant increase in carbon and hydrogen content for both modified materials. In addition, nitrogen was detected in SBA-15-APTES (Table 2).

Figure 1b shows the FTIR spectra of SBA-15, SBA-15-CD, and SBA-15-APTES. The materials exhibit a broad band at ~3400 cm^{-1}, characteristic of stretching vibrations of surface hydroxyl groups and adsorbed water, as well as a band at ~1630 cm^{-1} attributed to the bending vibrations of intra-structural water O–H groups. In the case of SBA-15-CD, additional bands were observed at ~2900 and 2860 cm^{-1}, attributed to asymmetric and symmetric stretching vibrations of C–H, $–CH_2$, and $–CH_3$ groups originating from the hydrocarbon moieties of the GLYMO linker and β-cyclodextrin. The band at ~1200 cm^{-1} can be attributed to Si–O–C stretching vibrations. These bands confirm the formation of covalent bonds between the silica structure and the linker, indicating successful modification. For SBA-15-APTES, two bands, at ~2900 cm^{-1} and ~1500 cm^{-1} correspond to characteristic aliphatic C–H stretching vibrations and N–H bending vibrations, respectively, confirming the presence of aminopropyl groups. In addition, the spectrum reveals characteristic bands of the silica structure, including Si–O–Si stretching at ~1100 cm^{-1} and symmetric stretching at ~800 cm^{-1} (Betiha et al., 2020).

The nitrogen sorption analysis (Figure 1c) confirms typical type IV isotherms with hysteresis loops for all tested samples, characteristic of mesoporous materials. SBA-15 exhibits the highest volume of adsorbed nitrogen, which reflects its large specific surface area and well-developed channel structure. After functionalization, a clear reduction in the volume of adsorbed gas is observed, with this effect being particularly pronounced in the case of SBA-15-CD. The reduction in the sorption signal indicates partial blockage of the mesopore channels by bulky cyclodextrin molecules. In the SBA-15-APTES sample, the decrease in N_2 adsorption is less pronounced, suggesting that the aminopropyl groups cover the pore walls without completely blocking them, thus leaving a significant part of the mesostructure accessible.

Table 2: Chemical composition of SBA-15 before and after functionalisation derived from XRF and CHN analyses

Material	Compound [%]					
	Al_2O_3	SiO_2	LOI	C	H	N
SBA-15	0.24	94.70	5.06	0.50	0.34	0.27
SBA-15-CD	0.37	79.69	19.91	12.19	2.95	0.77
SBA-15-APTES	0.25	87.87	11.82	6.10	2.38	2.07

LOI = Loss on ignition.

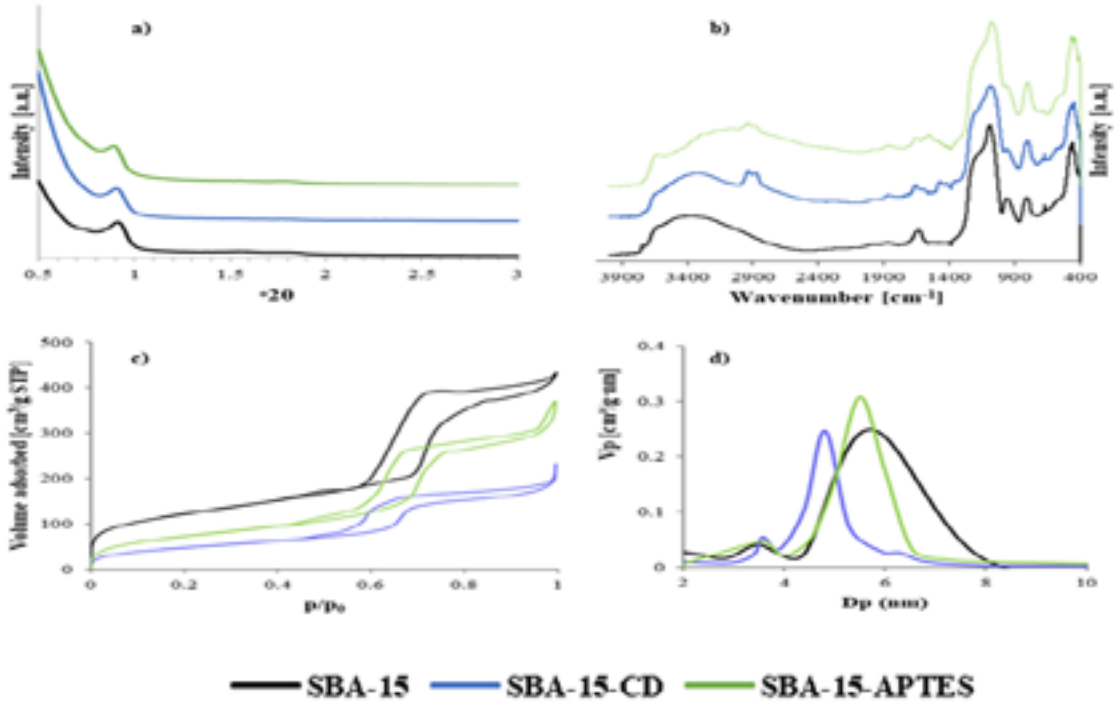

Fig. 1. Structural and textural characterization of SBA-15-based materials: (a) low-angle XRD patterns, (b) FTIR spectra, (c) N_2 adsorption–desorption isotherms, (d) pore size distributions calculated by BJH method. Pure SBA-15 (black), SBA-15-APTES (blue), SBA-15-CD (green)

The pore diameter distribution curves (Figure 1d) support these observations. SBA-15 is characterized by a narrow, symmetrical distribution with a maximum at approximately 5–6 nm, typical of ordered hexagonal mesopores. Modification with cyclodextrin leads to a shift of the maximum toward smaller diameters, indicating partial filling of the channels. In contrast, SBA-15-APTES exhibits a broader distribution shifted towards larger diameters, which may be associated with heterogeneous deposition of amino groups and local changes in channel geometry.

The summary of textural parameters (Table 3) clearly confirms the different effects of both functionalization strategies. SBA-15 is characterized by a high specific surface area (428 m^2/g), large pore volume (0.67 cm^3/g) and uniform mesoporosity. After functionalization with CD, the surface area and pore volume are significantly reduced (to 173 m^2/g and 0.29 cm^3/g), which is consistent with partial channel blockage. In the case of SBA-15-APTES, the reduction in textural parameters is clearly milder (265 m^2/g and 0.58 cm^3/g), while a widening of the pore diameter range is observed, suggesting a more heterogeneous structure.

In summary, both modifications were successfully carried out, but they differed in their effect on the material texture: cyclodextrin mainly reduced the available porosity, while amino groups preserved most of the mesostructure, although they made it more heterogeneous.

Figure 2 presents SEM images of the investigated materials. In the case of non-functionalized SBA-15, a characteristic homogeneous structure composed of ordered spherical aggregates is visible. After modification with cyclodextrin (SBA-15-CD), the structure becomes significantly more compact, and the grains form denser agglomerates with less distinct boundaries between particles. SBA-15-APTES retains the typical morphology of the original material, although small surface irregularities can be observed, consistent with the presence of grafted organosilane species. These observations are in line with the decrease in specific surface area and pore volume derived from the nitrogen adsorption isotherms. At

Table 3: Textural properties of SBA-15, SBA-15-CD, and SBA-15-APTES

Sample	S_{BET} (m^2/g)	V_{tot} (cm^3/g)	V_{mic} (cm^3/g)	V_{mes} (cm^3/g)	D_p (nm)
SBA-15	428	0.674	0.029	0.645	5.6-6.3
SBA-15-CD	173	0.293	---	0.293	4.9-6.6
SBA-15-APTES	265	0.579	---	0.579	6.9-8.3

Where: S_{BET} (m^2/g) – specific surface area; V_{tot} (cm^3/g) – total pore volume (at $p/p_0 \approx 0.99$); V_{mic} (cm^3/g) – micropore volume; V_{mes} (cm^3/g) – mesopore volume (calculated as the difference between V_{total} and V_{micro}); D_p (nm) – average pore diameter obtained from the BJH desorption method

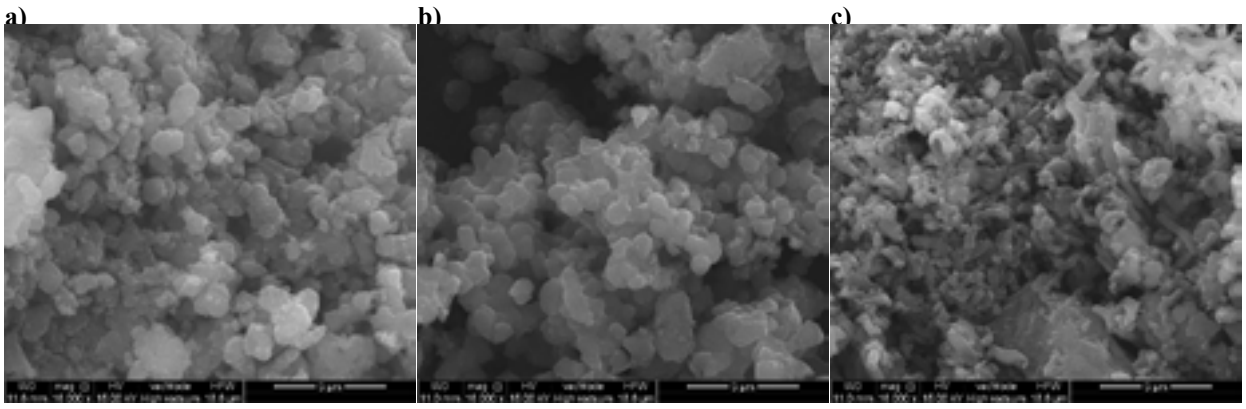

Fig. 2. SEM images of SBA-15 (a), SBA-15-CD (b), and SBA-15-APTES (c) at magnification 16000x

the same time, they indicate that the mesoporous character of SBA-15 is preserved in both modified samples.

Competitive adsorption performance of SBA-15-based adsorbents

Competitive adsorption of IBU, SMX, and TC on SBA-15-CD and SBA-15-APTES in the concentration range of 5–100 mg/L at pH 6.5 and 9.0 is shown in Figure 3a-d. In the case of a ternary system, standard isotherm models did not accurately describe the experimental data, suggesting a more complex co-adsorption mechanism. For this reason, the mechanistic analysis was based solely on empirical parameters (q_e, Kd, α). Table 4 presents the K_d and α coefficients determined for each material at both pH values and for selected C_0 levels (20, 40, 60, and 100 mg/L), where competitive effects were most pronounced. The results reveal clear differences in adsorption capacity and behavior in the ternary system, resulting from differences in the surface chemistry of the modified materials.

The selected pH values significantly influence the degree of pharmaceutical ionization and correspond to conditions typical of wastewater treatment systems. At both pH 6.5 and 9.0, IBU ($pK_a \approx 4.9$) occurs mainly in an anionic form. At around pH 6.5, SMX (pK_a 1.6 and 6.2) is present as a mixture of neutral and anionic forms, while at pH 9.0 it is predominantly deprotonated. TC is present mainly as a zwitterion at pH 6.5 and becomes negatively charged at pH 9.0.

The determined pH_{pzc} values were 6.2 for SBA-15-CD and 8.4 for SBA-15-APTES. This indicates that at pH 6.5 the SBA-15-CD surface is close to neutral, limiting electrostatic interactions, while SBA-15-APTES remains positively charged favoring electrostatic attraction toward anionic species. At pH 9.0, both adsorbents are negatively charged, leading to electrostatic repulsion toward all pharmaceuticals. However, SBA-15-CD maintains relatively high performance due to the dominance of non-electrostatic interactions such as host–guest inclusion and H-bonding/π–π interactions, which also explains the increased relative adsorption of TC at higher concentrations.

SBA-15-CD exhibited the highest adsorption capacity at both pH values. At C_0 = 100 mg/L and pH 6.5, the q_e capacities

Table 4: Distribution (Kd) and selectivity (α) coefficients of IBU, SMX and TC in ternary systems at selected C0 for SBA-15-CD and SBA-15-APTES

pH	Adsorbent	C_0 (mg/L)	K_{d_IBU} (L/g)	K_{d_SMX} (L/g)	K_{d_TC} (L/g)	$\alpha_{TC/IBU}$	$\alpha_{TC/SMX}$	$\alpha_{SMX/IBU}$
6.5	SBA-15-CD	10	504.12	504.12	94.38	0.19	0.19	1.00
		20	23.09	48.19	34.50	1.49	0.72	1.16
		60	37.50	32.42	31.93	0.85	0.99	0.86
		100	5.48	5.91	29.13	5.31	4.93	1.08
	SBA-15-APTES	10	502.02	502.02	29.00	0.06	0.06	1.00
		20	10.31	17.51	15.39	1.49	0.88	1.70
		60	1.73	3.27	12.38	7.17	3.79	1.89
		100	0.46	0.65	0.31	0.69	0.48	1.42
9.0	SBA-15-CD	10	502.31	502.31	181.38	0.36	0.36	1.00
		20	24.37	13.23	41.70	1.71	3.15	0.54
		60	19.90	16.67	29.29	1.47	1.76	0.84
		100	5.53	6.94	19.79	3.58	2.85	1.26
	SBA-15-APTES	10	88.56	496.21	22.91	0.26	0.05	5.60
		20	10.95	3.28	8.04	0.73	2.45	0.30
		60	1.56	1.04	0.72	0.46	0.69	0.67
		100	0.44	0.63	0.77	1.75	1.23	1.43

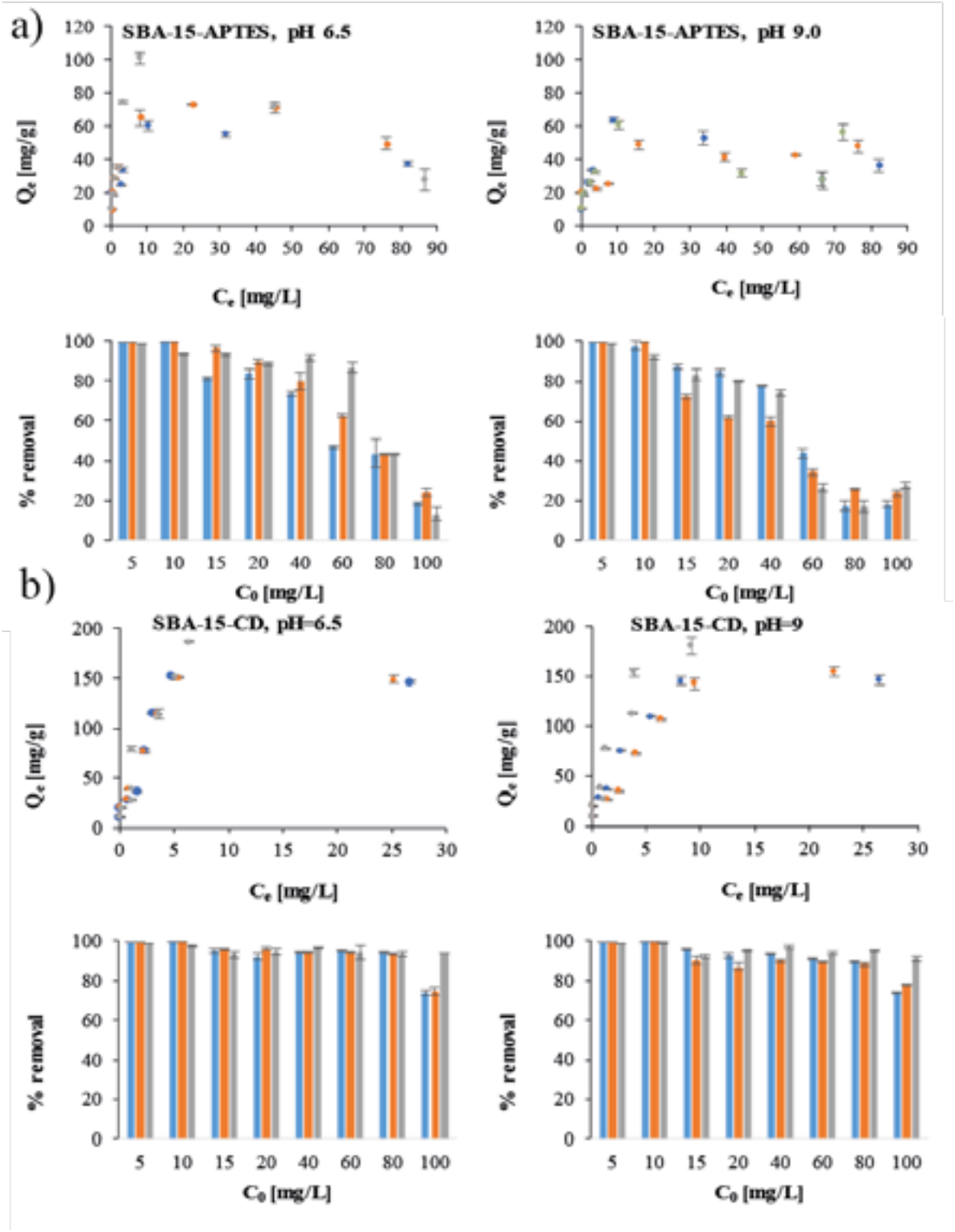

Fig. 3. Qe vs. Ce plots and percentage removal (%) at pH 6.5 and 9.0 of IBU, SMX, and TC from ternary mixtures on SBA-15-APTES (a), and SBA-15-CD (b).

were 146.7 mg/g (IBU), 142.9 mg/g (SMX), and 159.4 mg/g (TC), with removal efficiencies exceeding 90% across most of the concentration range. Similarly high capacities (146 – 181 mg/g) were observed at pH 9.0, indicating relatively stable adsorption performance over a broad pH range. This behavior is consistent with reports for cyclodextrin-functionalized and hybrid SBA-15 systems, where combined host–guest inclusion and hydrogen bonding interactions stabilize sorption over a wide pH range (Demircan Ozelcaglayan et al., 2024; Zhou et al., 2024).

In contrast, SBA-15-APTES achieved lower adsorption capacities, particularly at pH 9.0, which may be attributed to the reduced protonation of $–NH_2$/$–NH_3^+$ groups (pKa ≈ 9–10), weakening electrostatic interactions (Zhang et al., 2015). The strong dependence of pharmaceutical sorption on pH, resulting from changes in the degree of ionization and surface charge of

the adsorbent, is widely reported for antibiotics and NSAIDs on carbon adsorbents, biochars, and mesoporous silicas (Otalvaro et al., 2019; Wang et al., 2020).

At low C_0 (≤10 mg/L), both materials showed nearly complete removal of all the pharmaceuticals, corresponding to conditions where the number of available active sites exceeds the number of adsorbate molecules. In this range, adsorption is governed primarily by affinity-driven interactions, and IBU and SMX exhibit higher apparent affinity than TC, as reflected by higher K_d values. Therefore, preferential adsorption of TC is not observed under low concentration conditions.

At $C_0 \geq 20$ mg/L, competitive effects become significant, which is reflected by K_d and α coefficients. For SBA-15-CD, TC adsorption becomes progressively more pronounced with increasing concentration, especially at C_0 = 100 mg/L, where it dominates relative to IBU and SMX ($\alpha_{-TC/IBU}$ and $\alpha_{-TC/SMX} > 1$). This indicates that TC preference is clearly concentration-dependent and emerges primarily under competitive, high-loading conditions. Furthermore, SBA-15-CD exhibits similar affinity toward IBU and SMX over most of the investigated concentration range, suggesting competition for similar adsorption sites.

In contrast, SBA-15-APTES shows less consistent selectivity patterns, reflecting a more heterogeneous surface and stronger sensitivity to pH. Although partial TC preference is observed under selected conditions (e.g., $\alpha_{-TC/IBU}$ = 1.75 at pH=9.0), the overall adsorption capacity remains significantly lower than for SBA-15-CD.The concentration-dependent shift in α values thus quantitatively reflects the transition from affinity-controlled uptake at low C_0 to site competition and steric exclusion at high C_0, as commonly observed in multisolute PPCP systems (Ahmed et al., 2017; Jin et al., 2023).

The unique performance of SBA-15-CD can be attributed to the synergy of multiple interaction mechanisms: (1) inclusion complexation within the β-cyclodextrin cavity (independent of pH), and (2) hydrogen bonding and π–π interactions between CD functional groups and drug molecules. TC, as a polyfunctional and conformationally flexible molecule, can engage in multiple simultaneous interactions, including hydrogen bonding, π–π stacking, and host–guest inclusion, favoring its dominance under competitive conditions (Demircan Ozelcaglayan et al., 2024; García-Criado et al., 2025). In contrast, IBU and SMX, with simpler molecular structures and fewer interaction modes, exhibit similar adsorption behavior. The relatively pH-independent performance of SBA-15-CD indicates that non-electrostatic interactions (host–guest inclusion and H-bonding/π–π interactions) dominate over purely electrostatic contributions.

The adsorption mechanism of SBA-15-APTES is based mainly on electrostatic interactions and hydrogen bonding. At pH 6.5, $–NH_3^+$ groups dominate, promoting binding of anionic species, whereas at pH 9.0, their degree of protonation decreases, weakening electrostatic interactions and reducing sorption capacity. The sharp capacity decrease at pH 9.0 is consistent with reports for amine-functionalized SBA-15, where deprotonation of $–NH_3^+$ groups suppresses anion binding despite unchanged textural properties (Derylo-Marczewska et al., 2023). However, in ternary systems, the effective uptake reflects both electrostatic contributions and steric/competitive effects. Overall, competitive adsorption in the ternary system is governed by the balance between electrostatic attraction/repulsion, host–guest inclusion, and specific H-bonding/π–π interactions, modulated by solute speciation and surface charge.

Table 5 summarizes the sorption of IBU, SMX, and TC and compares the obtained results with literature data, including key parameters such as adsorbent dose, initial concentration (C_0), adsorption capacity (q_e), and removal efficiency. The results show that SBA-15-CD and SBA-15-APTES achieve high adsorption capacities and removal efficiencies that are comparable to or higher than those reported for other adsorbents, despite the multicomponent conditions. The relatively high performance observed in the ternary system may suggest the contribution of co-adsorption or other synergistic effects, as reported in the literature for complex adsorption systems (Siratham et al., 2025).

Conclusions

This paper presents the adsorption efficiency of mesoporous silica SBA-15 modified with β-CD and APTES with respect to IBU, SMX, and TC in a ternary aqueous system. The adsorbents were synthesized using waste solution obtained after the synthesis of zeolites from fly ash as a silicon source. The results of the material characterization showed that waste-derived SBA-15 was characterized by high purity, a well-developed specific surface area, and an ordered hexagonal pore structure. The structure of the silica carrier remained intact after modification, while the observed changes in surface chemistry, morphology, and texture (SEM, N_2 isotherm, CHN, FTIR) confirmed the successful introduction of functional groups and the resulting changes in surface properties.

The hybrid materials SBA-15-CD and SBA-15-APTES showed high efficiency in removing the tested pharmaceuticals, especially at lower initial concentrations. At the same time, significant differences in the adsorption mechanism and pH-dependent stability were observed. SBA-15-CD exhibited significantly higher sorption efficiency than SBA-15-APTES. At pH 6.5, the highest sorption capacities (q_e) for SBA-15-CD were 151.7 mg/g for IBU, 150.4 mg/g for SMX, and 186.5 mg/g for TC, whereas for SBA-15-APTES they were 81.8, 47.9, and 100.9 mg/g, respectively. Furthermore, SBA-15-CD maintained similar removal efficiency at pH 9.0, whereas SBA-15-APTES showed a significant decrease in efficiency at C_0>60 mg/L, ranging from 26% to 60%, depending on the compound.

These differences result from distinct interaction mechanisms: for SBA-15-CD, host-guest inclusion complexation and hydrophobic interactions dominate, while for SBA-15-APTES, adsorption is mainly governed by electrostatic interactions, which weaken at higher pH due to reduced protonation of amino groups. The high adsorption efficiency of SBA-15-CD in the presence of a mixture of pharmaceuticals and its stability within the pH range typical of wastewater (6.5–9.0) indicate its strong potential for the removal of micropollutants from real water matrices. At the same time, the use of a post-synthesis waste stream as a silicon source is consistent with the principles of the circular economy.

Acknowledgement

The work was carried out as part of the project entitled “Sorption of organic micropollutants on cyclodextrin-

Table 5: Comparative adsorption of IBU, SMX and TC on selected adsorbents

Compound	Adsorbent	Dose (g/L)	C_0 (mg/L)	Sorption Capacity (mg/g)	Removal (%)	Conditions	Reference
IBU, TC	Rice husk and peach stone activated carbons (AC-RH, AC-PS)	0.5	10–200 (batch); 120 (fixed-bed)	IBU: q_{max} = 239.8; TC: q_{max} = 845.9	~96–97 (column breakthrough)	Fixed-bed, single, model water	(Álvarez-Torrellas et al. 2015)
IBU, SMX	Magnetic orange-peel biochar (Fe_3O_4-modified)	1.0	0.5–100	IBU: $q_{max} \approx 60$; SMX: $q_{max} \approx 40$	>90 ($C_0 \leq 20$ mg/L)	Single, model water	(Ai et al. 2020)
SMX, TC	$MgFe_2O_4$-magnetic biochar	0.2	5–100	SMX: q_{max} = 50.75; TC: q_{max} = 120.36	>90 ($C_0 \leq$ 20–25 mg/L)	Single/binary, model water (pH, ions, DOM)	(Deng et al. 2022)
TC	KOH/$KMnO_4$-modified biochar (K-Mn-BC)	0.2	5–200	q_{max} = 584.19	>95 ($C_0 \approx$ 50 mg/L)	Single, model water	(Xu et al. 2022)
SMX, LIN	H_3PO_4-modified sludge biochar (PBC)	1.0	5–80	SMX: q_{max} = 45.6	>90 ($C_0 \leq$ 40 mg/L)	Single/binary, model & real water	(Minaei et al. 2024)
IBU, SMX	Corn starch nanoparticles (CSNP)	1.0	10	$q_e \approx$ 0.86 (each)	~86	Binary, model water	(Priyan V and Narayanasamy 2022)
IBU	Chitosan-modified waste tire crumb rubber	3.0	30	q_e = 17.7	~50	Single, real water (spiked)	(Phasuphan et al. 2019)
IBU, SMX, TC	SBA-15-CD	0.5	5–100	IBU: q_e = 151.71; SMX: q_e = 154.85; TC: q_e = 186.46	IBU: 93–99; SMX: 89–99; TC: 96–98 ($C_0 \leq$ 40 mg/L)	Ternary, pH 6.5 & 9.0, model water	This study
IBU, SMX, TC	SBA-15-APTES	0.5	5–100	IBU: q_e = 71.03; SMX: q_e = 73.15; TC: q_e = 100.89	IBU: 73–99; SMX: 59–99; TC: 74–98 ($C_0 \leq$ 40 mg/L)	Ternary, pH 6.5 & 9.0, model water	This study

modified synthetic zeolites and zeolite-carbon composites from fly ash" No. BPN/BEK/ 2021/2/00019, financed by the National Agency for Academic Exchange (NAWA) under the Mieczysław Bekker Program.

References

Abegunde, S.M., Idowu, K.S., Adejuwon, O.M. & Adeyemi-Adejolu, T. (2020). A review on the influence of chemical modification on the performance of adsorbents. *Resources, Environment and Sustainability* 1, 100001. DOI:10.1016/j.resenv.2020.100001

Abukhadra, M.R. (2024). Steric, Synergetic, Energetic Studies on the Impact of the Type of the Hybridized Polymers (Chitosan and β-Cyclodextrin) on the Adsorption Properties of Zeolite-A for Congo Red Dye. DOI:10.1021/acsomega.4c01134

Acharya, A., Jeppu, G., Raju Girish, C. & Prabhu, B. (2023). Development of a Multicomponent Adsorption Isotherm Equation and Its Validation by Modeling. *Langmuir* 39, pp. 17862–17878. DOI:10.1021/acs.langmuir.3c02496

Ahmed, M.B., Zhou, J.L., Ngo, H.H., Guo, W., Johir, M.A.H. & Sornalingam, K. (2017). Single and competitive sorption properties and mechanism of functionalized biochar for removing sulfonamide antibiotics from water. *Chemical Engineering Journal* 311, pp. 348–358. DOI:10.1016/j.cej.2016.11.106

Ai, T., Jiang, X., Zhong, Z., Li, D. & Dai, S. (2020). Methanol-modified ultra-fine magnetic orange peel powder biochar as an effective adsorbent for removal of ibuprofen and sulfamethoxazole from water. *Adsorption Science & Technology* 38, pp. 304–321. DOI:10.1177/0263617420944659

Ajaz, S., Aly Hassan, A., Michael, R.N. & Leusch, F.D.L. (2024). Removal of organic micropollutants in biologically active filters: A systematic quantitative review of key influencing factors. *Journal of Environmental Management* 353, 120203. DOI:10.1016/j.jenvman.2024.120203

Althumayri, K., Guesmi, A., El-Fattah, W.A., Houas, A., Hamadi, N.B. & Shahat, A. (2023). Enhanced Adsorption and Evaluation of Tetracycline Removal in an Aquatic System by Modified Silica Nanotubes. *ACS Omega* 8, pp. 6762–6777. DOI:10.1021/acsomega.2c07377

Álvarez-Torrellas, S., Rodríguez, A., Ovejero, G. & García, J. (2015). Comparative adsorption performance of ibuprofen and tetracycline from aqueous solution by carbonaceous materials. *Chemical Engineering Journal* 283, pp. 936–947. DOI:10.1016/j.cej.2015.08.023

Amalina, F., Razak, A.S.A., Krishnan, S., Zularisam, A.W. & Nasrullah, M. (2022). The effects of chemical modification on adsorbent performance on water and wastewater treatment - A review. *Bioresource Technology Reports* 20, 101259. DOI:10.1016/j.biteb.2022.101259

Baigorria, E., Carvalho, L.B., Alves Pinto, L.M. & Fraceto, L.F. (2024). Cyclodextrin–silica hybrid materials: synthesis, characterization, and application in pesticide aqueous removal. *Front. Chem*. 12. DOI:10.3389/fchem.2024.1450089

Bandura, L., Białoszewska, M., Leiviskä, T. & Franus, W. (2022). The Role of Zeolite Structure in its B-Cyclodextrin Modification and Tetracycline Adsorption from Aqueous Solution: Characteristics and Sorption Mechanism. *SSRN Electronic Journal.* DOI:10.2139/ssrn.4153170

Bandura, L., Białoszewska, M., Malinowski, S. & Franus, W. (2021). Adsorptive performance of fly ash-derived zeolite modified by β-cyclodextrin for ibuprofen, bisphenol A and caffeine removal from aqueous solutions – equilibrium and kinetic study. *Applied Surface Science* 150160–150160. DOI:10.1016/j.apsusc.2021.150160

Betiha, M.A., Moustafa, Y.M., El-Shahat, M.F. & Rafik, E. (2020). Polyvinylpyrrolidone-Aminopropyl-SBA-15 schiff Base hybrid for efficient removal of divalent heavy metal cations from wastewater. *Journal of Hazardous Materials*, 397, 122675. DOI:10.1016/j.jhazmat.2020.122675

Caicedo, D.F., dos Reis, G.S., Lima, E.C., De Brum, I.A.S., Thue, P.S., Cazacliu, B.G., Lima, D.R., dos Santos, A.H. & Dotto, G.L. (2020). Efficient adsorbent based on construction and demolition wastes functionalized with 3-aminopropyltriethoxysilane (APTES) for the removal ciprofloxacin from hospital synthetic effluents. *Journal of Environmental Chemical Engineering* 8, 103875. DOI:10.1016/j.jece.2020.103875

Cavalcante, E.H.M., Candido, I.C.M., de Oliveira, H.P., Silveira, K.B., Víctor de Souza Álvares, T., Lima, E.C., Thyrel, M., Larsson, S.H. & Simões dos Reis, G. (2022). 3-Aminopropyl-triethoxysilane-Functionalized Tannin-Rich Grape Biomass for the Adsorption of Methyl Orange Dye: Synthesis, Characterization, and the Adsorption Mechanism. *ACS Omega 7*, 18997–19009. DOI:10.1021/acsomega.2c02101

Demircan Ozelcaglayan, E., Honek, J.F. & Parker, W.J. (2024). Molecular level investigation of interactions between pharmaceuticals and β-cyclodextrin (β-CD) functionalized adsorption sites for removal of pharmaceutical contaminants from water. *Chemosphere*, 347, 140639. DOI:10.1016/j.chemosphere.2023.140639

Deng, Y., Wang, M., Yang, Y., Li, X., Chen, W. & Ao, T. (2022). Enhanced adsorption performance of sulfamethoxazole and tetracycline in aqueous solutions by MgFe2O4-magnetic biochar. *Water Sci Technol* 86, pp. 568–583. DOI:10.2166/wst.2022.227

Derylo-Marczewska, A., Zienkiewicz-Strzalka, M., Kusmierek, K., Skrzypczynska, K. & Swiatkowski, A. (2023). Effect of the SBA-15 N-functionalization on the adsorption of organic contaminants. *Desalination and Water Treatment*, 312, pp. 39–49. DOI:10.5004/dwt.2023.29947

Flores, D., Almeida, C.M.R., Gomes, C.R., Balula, S.S. & Granadeiro, C.M. (2023). Tailoring of Mesoporous Silica-Based Materials for Enhanced Water Pollutants Removal. *Molecules*, 28, 4038. DOI:10.3390/molecules28104038

García-Criado, N., Martín-Pozo, L., Martín, J., Santos, J.L., Aparicio, I. & Alonso, E. (2025). Efficient Removal of Tetracyclines and Their Metabolites from Wastewater Using Purified Stevensite: Adsorption Capacity, Reusability, and Antibiotic Decontamination. *Antibiotics* 14, 395. DOI:10.3390/antibiotics14040395

Huynh, N.C., Nguyen, T.T.T., Nguyen, D.T.C. & Tran, T.V. (2023). Occurrence, toxicity, impact and removal of selected non-steroidal anti-inflammatory drugs (NSAIDs): A review. *Science of The Total Environment*, 898, 165317. DOI:10.1016/j.scitotenv.2023.165317

Jin, R., Zhao, C., Song, Y., Qiu, X., Li, C. & Zhao, Y. (2023). Competitive adsorption of sulfamethoxazole and bisphenol A on magnetic biochar: Mechanism and site energy distribution. *Environmental Pollution*, 329, 121662. DOI:10.1016/j.envpol.2023.121662

Kilpinen, K., Tisler, S., Jørgensen, M.B., Mortensen, P. & Christensen, J.H. (2024). Temporal trends and sources of organic

micropollutants in wastewater. *Science of The Total Environment,* 957, 177555. DOI:10.1016/j.scitotenv.2024.177555

Kim, J.-P., Jin, D.R., Lee, W., Chae, M. & Park, J. (2020). Occurrence and Removal of Veterinary Antibiotics in Livestock Wastewater Treatment Plants, South Korea. *Processes*, 8, 720. DOI:10.3390/pr8060720

Lagiewka, J., Pajdak, A. & Zawierucha, I. (2025). Adsorption performance and mechanism of a novel composite based on β-cyclodextrin polymer and chitosan: Selective and rapid removal of acid orange 7. *Carbohydrate Polymers*, 353, 123297. DOI:10.1016/j.carbpol.2025.123297

Mallard, I., Städe, L.W., Ruellan, S., Jacobsen, P.A.L., Larsen, K.L. & Fourmentin, S. (2015). Synthesis, characterization and sorption capacities toward organic pollutants of new β-cyclodextrin modified zeolite derivatives. *Colloids and Surfaces A: Physicochemical and Engineering Aspects*, 482, pp. 50–57. DOI:10.1016/j.colsurfa.2015.04.014

Minaei, S., Zoroufchi Benis, K., McPhedran, K.N. & Soltan, J. (2024). Adsorption of sulfamethoxazole and lincomycin from single and binary aqueous systems using acid-modified biochar from activated sludge biomass. *Journal of Environmental Management* ,358, 120742. DOI:10.1016/j.jenvman.2024.120742

Mohassel Yazdi, N. & Naimi-Jamal, M.R. (2024). One-pot synthesis of quinazolinone heterocyclic compounds using functionalized SBA-15 with natural material ellagic acid as a novel nanocatalyst. *Scientific Reports*, 14, 11189. DOI:10.1038/s41598-024-61803-y

Nguyen, Q.K., Phan, T.T.T., Tran, N.B., Tran, D.D., Nguyen, T.M., Pham, B., Nguyen, T.A.H., Pham, D.T. & Pham, T.N.M. (2025). Enhanced adsorption of sulfamethoxazole antibiotic on amine grafted activated carbon using (3-Aminopropyl) triethoxysilane (APTES). *Materials Chemistry and Physics*, 339, 130782. DOI:10.1016/j.matchemphys.2025.130782

Otalvaro, J.O., Avena, M. & Brigante, M. (2019). Adsorption of organic pollutants by amine functionalized mesoporous silica in aqueous solution. Effects of pH, ionic strength and some consequences of APTES stability. *Journal of Environmental Chemical Engineering*, 7, 103325. DOI:10.1016/j.jece.2019.103325

Panek, R., Madej, J., Bandura, L. & Słowik, G. (2021). Recycling of Waste Solution after Hydrothermal Conversion of Fly Ash on a Semi-Technical Scale for Zeolite Synthesis. *Materials*, 14, 1413. DOI:10.3390/ma14061413

Phasuphan, W., Praphairaksit, N. & Imyim, A. (2019). Removal of ibuprofen, diclofenac, and naproxen from water using chitosan-modified waste tire crumb rubber. *Journal of Molecular Liquids*, 294, 111554. DOI:10.1016/j.molliq.2019.111554

Poulson, B.G., Alsulami, Q.A., Sharfalddin, A., El Agammy, E.F., Mouffouk, F., Emwas, A.-H., Jaremko, L. & Jaremko, M. (2022). Cyclodextrins: Structural, Chemical, and Physical Properties, and Applications. *Polysaccharides,* 3, pp. 1–31. DOI:10.3390/polysaccharides3010001

Priyan V, V. & Narayanasamy, S. (2022). Effective removal of pharmaceutical contaminants ibuprofen and sulfamethoxazole from water by Corn starch nanoparticles: An ecotoxicological assessment. *Environmental Toxicology and Pharmacology*, 94, 103930. DOI:10.1016/j.etap.2022.103930

Samal, K., Mahapatra, S. & Hibzur Ali, M. (2022). Pharmaceutical wastewater as Emerging Contaminants (EC): Treatment technologies, impact on environment and human health. *Energy Nexus*, 6, 100076. DOI:10.1016/j.nexus.2022.100076

Sim, W.-J., Lee, J.-W., Lee, E.-S., Shin, S.-K., Hwang, S.-R. & Oh, J.-E. (2011). Occurrence and distribution of pharmaceuticals in wastewater from households, livestock farms, hospitals and pharmaceutical manufactures. *Chemosphere,* 82, pp. 179–186. DOI:10.1016/j.chemosphere.2010.10.026

Siratham, S., Osathaphan, K. & Punyapalakul, P. (2025). Competitive adsorption of pharmaceuticals and dissolved organic matter from hospital effluent on amine-functionalized periodic mesoporous organosilicas. *Sci Rep*., 15, 34454. DOI:10.1038/s41598-025-17629-3

Syeda, S.E.Z., Nowacka, D., Khan, M.S. & Skwierawska, A.M. (2022). Recent Advancements in Cyclodextrin-Based Adsorbents for the Removal of Hazardous Pollutants from Waters. *Polymers*, 14, 2341. DOI:10.3390/polym14122341

Tang, Y., Gomi, R., Takeuchi, H., Nishimura, F. & Ihara, M. (2025). Occurrence of antibiotics and antibiotic-resistant bacteria in a Japanese city revealed by wastewater surveillance in the sewer system. *Water Research*, 285, 124136. DOI:10.1016/j.watres.2025.124136

Walsh, T.R., Gales, A.C., Laxminarayan, R. & Dodd, P.C. (2023). Antimicrobial Resistance: Addressing a Global Threat to Humanity. *PLOS Medicine*, 20, e1004264. DOI:10.1371/journal.pmed.1004264

Wang, B., Xu, X., Tang, H., Mao, Y., Chen, H. & Ji, F. (2020). Highly efficient adsorption of three antibiotics from aqueous solutions using glucose-based mesoporous carbon. *Applied Surface Science*, 528, 147048. DOI:10.1016/j.apsusc.2020.147048

Wang, M.-L., He, Z.-F. & Wang, J.-C. (2025). B-Cyclodextrin-Based Porous Organic Polymers for the Removal of Environmental Pollutants from Water. *Computer Fraud and Security*, pp. 1081–1087. DOI:10.52710/cfs.447

Włodarczyk-Makuła, M. (2024). Selected organic micropollutants in the aquatic environment. *Desalination and Water Treatment*, 317, 100061. DOI:10.1016/j.dwt.2024.100061

Xiang Chuin, L., Kamaruzaman, S., Mangala Praveena, S. & Yahaya, N. (2024). Recent applications of β-cyclodextrin in selective adsorption of pesticides, heavy metals, and organic pollutants from water samples: Mini review. *Microchemical Journal*, 206, 111583. DOI:10.1016/j.microc.2024.111583

Xu, J., Zhang, Y., Li, B., Fan, S., Xu, H. & Guan, D.-X. (2022). Improved adsorption properties of tetracycline on KOH/KMnO4 modified biochar derived from wheat straw. *Chemosphere*, 296, 133981. DOI:10.1016/j.chemosphere.2022.133981

Zhang, Z., Lan, H., Liu, H. & Qu, J. (2015). Removal of tetracycline antibiotics from aqueous solution by amino-Fe (III) functionalized SBA15. *Colloids and Surfaces A: Physicochemical and Engineering Aspects*, 471, pp. 133–138. DOI:10.1016/j.colsurfa.2015.02.018

Zhou, Y., Wang, J., Yang, J., Duan, L.-H., Liu, H.-B., Wu, J. & Gao, L. (2024). Mesoporous Silica-Confined MOF-525 for Stable Adsorption of Tetracycline over a Wide pH Application Range. *ACS Appl. Nano Mater*., 7, pp. 3806–3816. DOI:10.1021/acsanm.3c05407

Konkurencyjna adsorpcja farmaceutyków z roztworów wieloskładnikowych na funkcjonalizowanej mezoporowatej krzemionce: porównanie modyfikacji powierzchni β-cyklodekstryną i aminą

Streszczenie. W artykule porównano skuteczność usuwania ibuprofenu (IBU), sulfametoksazolu (SMX) i tetracykliny (TC) z mieszaniny tych substancji przy użyciu mezoporowatej krzemionki SBA-15 modyfikowanej β-cyklodekstryną (CD) i aminosilanem (APTES). SBA-15 został zsyntetyzowany przy użyciu roztworu odpadowego pochodzącego z syntezy zeolitów z popiołu lotnego jako źródła krzemu. W celu uzyskania charakterystyki strukturalnej, chemicznej i powierzchniowej materiałów hybrydowych przeprowadzono dyfrakcję rentgenowską (XRD), analizę elementarną CHN, spektroskopię w podczerwieni Fouriera (FT-IR), izotermę adsorpcji N_2 oraz skaningową mikroskopię elektronową (SEM). Przeprowadzono testy adsorpcji wsadowej w celu oceny oddziaływań między adsorbentem a adsorbatem oraz konkurencji adsorbentów przy pH 6,5 i 9,0. pośród badanych farmaceutyków preferencyjnie adsorbowany był TC, co wskazuje na jego wyższe powinowactwo wynikające z obecności wielu grup funkcyjnych umożliwiających oddziaływanie z powierzchnią adsorbentów. Maksymalna wartość pojemności sorpcyjnej qe dla TC wynosiła 186,5 mg/g i 100,9 mg/g odpowiednio dla SBA-15-CD i SBA-15-APTES, podczas gdy qe dla IBU i SMX była na podobnym poziomie i wynosiła ~ 150 mg/g i ~ 71 mg/g przy pH 6,5. SBA-15-CD wykazał podobną skuteczność usuwania przy obu badanych wartościach pH, podczas gdy SBA-15-APTES wyraźnie stracił swoje powinowactwo do adsorbentów przy pH 9,0, gdzie qe spadło o około 20% dla SMX w porównaniu z pH 6,5. Wyniki wskazują na wysoki potencjał funkcjonalizowanego SBA-15 pochodzącego z odpadów w oczyszczaniu wody i ścieków zanieczyszczonych substancjami farmaceutycznymi.